Supporting Information

Coordination Engineering of Nickel Sites in Ni-MOF for Synergistic Optimization of Electronic Structure and Interfacial Water toward Efficient Alkaline Hydrogen Evolution

Jiayi Wang [1], Yitao Ouyang [1],Qing Liao [1], Xiufeng Yi [1], Yi Wei[1], Weijie Li [2], Chao Han [1]*

1. School of Materials Science and Engineering, Key Laboratory of Electronic Packaging and Advanced Functional Materials of Hunan Province, Central South University, Changsha, 410083, Hunan, China

2. Powder Metallurgy Research Institute, Central South University, Changsha 410083, Hunan Province, P. R. China

I. Supplementary figures and tables

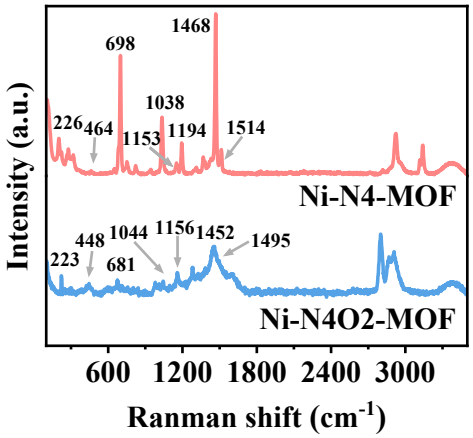

Figure S1. Raman spectrum of Ni-N4-MOF and Ni-N4O2-MOF.

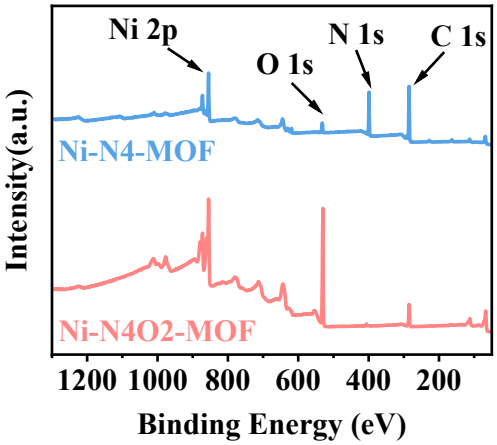

Figure S2. XPS spectra of survey scan of Ni-N4-MOF and Ni-N4O2-MOF.

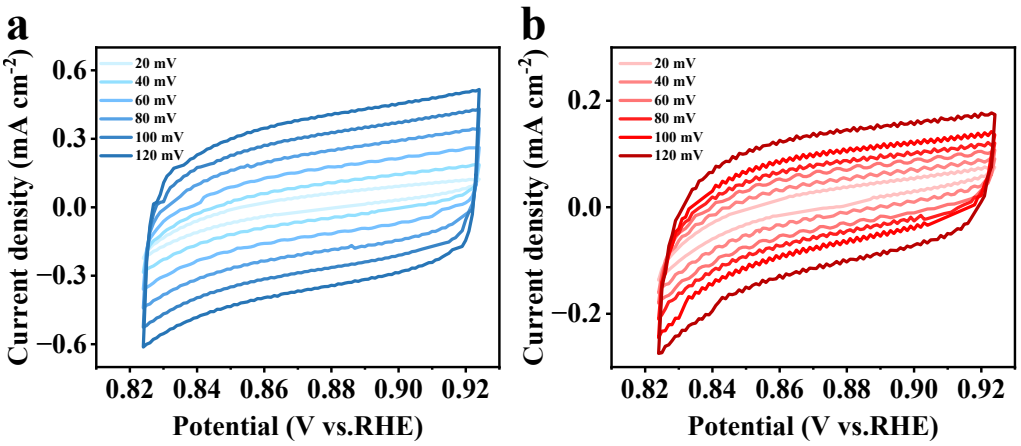

Figure S3. Electrochemical CV scans of (a) Ni-N4-MOF and (b) Ni-N4O2-MOF.

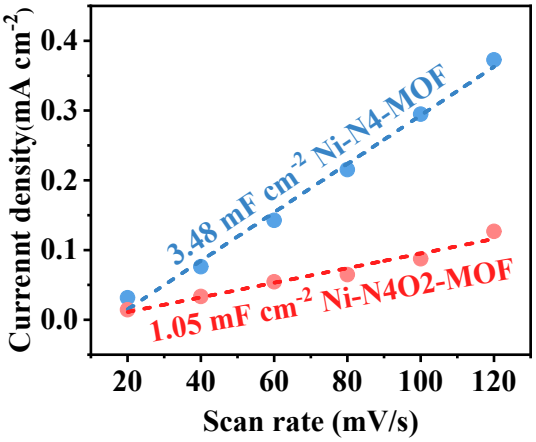

Figure S4. Calculated double layers capacitances extracted from the linear fitting of the capacitive currents versus CV scan rates for Ni-N4-MOF and Ni-N4O2-MOF.

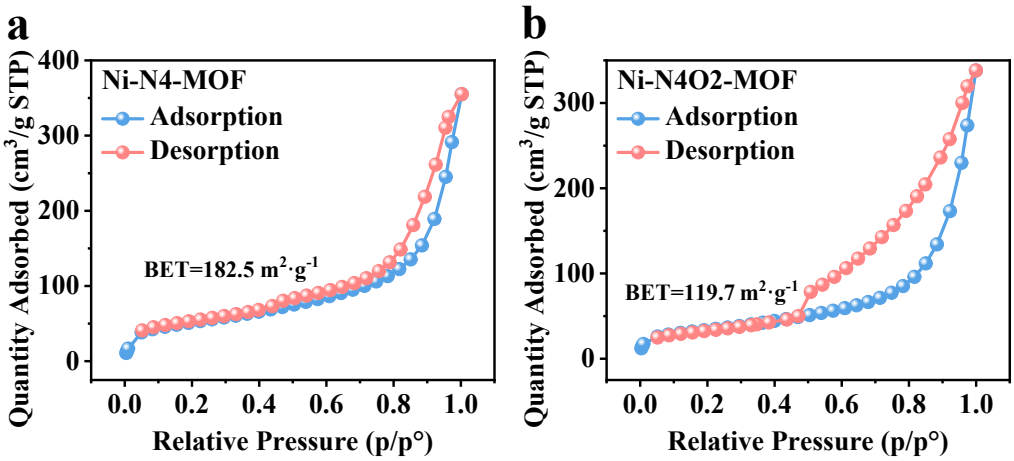

Figure S5. N_2 adsorption-desorption isotherm. (a) Ni-N4-MOF and (b) Ni-N4O2-MOF and the corresponding specific surface areas as estimated from Brunauer-Emmett-Teller (BET) measurements.

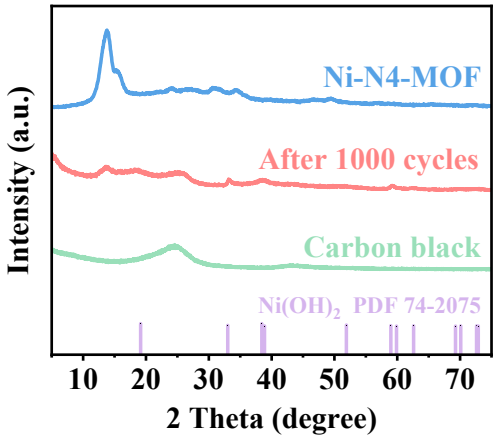

Figure S6. The XRD pattern of Ni-N4-MOF after the ADTs.

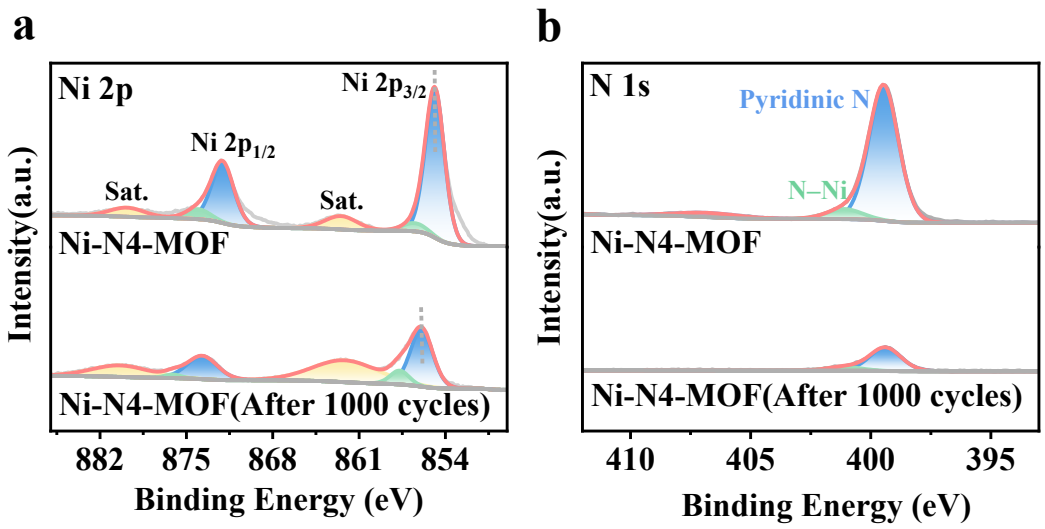

Figure S7. High-resolution XPS spectra of a) Ni 2p and b) N 1s for Ni-N4-MOF and Ni-N4-MOF(After 1000 cycles).

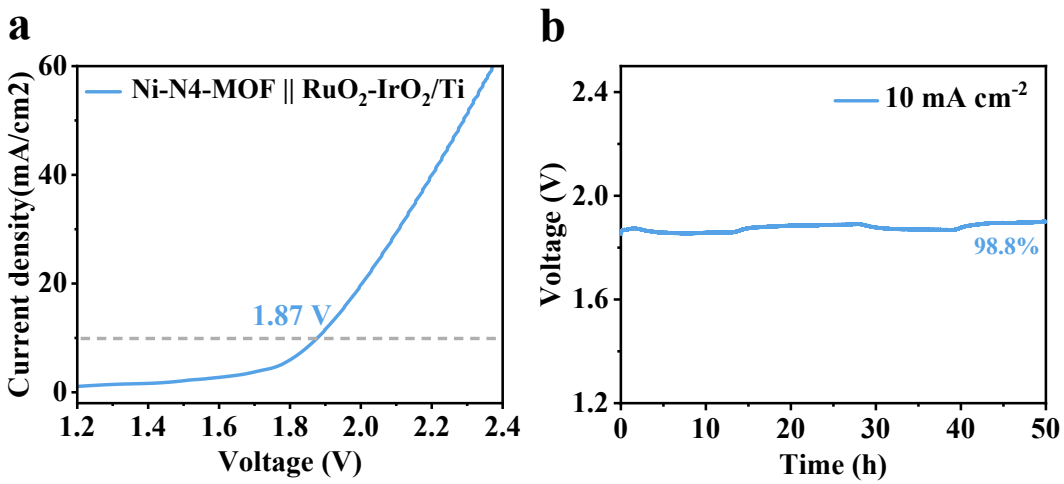

Figure S8. a) LSV curves of Ni-N4-MOF || RuO_2-IrO_2/Ti systems. b) Stability test of Ni-N4-MOF || RuO_2-IrO_2/Ti electrode for overall water splitting.

To maintain consistency in testing before and after the experiment, a rotating disk electrode was also used in this test. The small fluctuations in the chronopotentiometric curve are mainly attributed to the periodic detachment of bubbles from the rotating disk electrode, as well as the slight evolution of the RuO_2-IrO_2/Ti anode surface. The overall voltage trend remains stable.

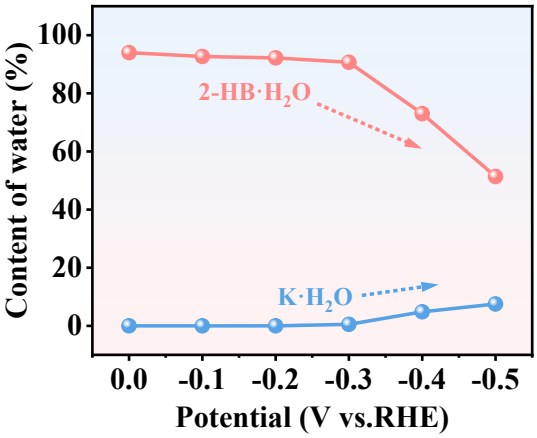

Figure S9. Change in peak area content of 2-HB·H_2O and K·H_2O for Ni-N4O2-MOF from -0.16 to -0.52 V *vs*. RHE.

Table S1. EXAFS fitting parameters at the Ni K-edge for Ni-MOFs

Sample	Shell	R (Å)	CN	σ^2 ($Å^2$)	R-factor
Ni-N4-MOF	Ni-N	1.89±0.01	4.4±0.7	0.004±0.002	0.009
	Ni-C	2.83±0.02	4.4±1.3	0.003±0.001	
Ni-N4O2-MOF	Ni-N/O	2.06±0.02	5.7±1.0	0.005±0.004	0.017
	Ni-Ni	2.44±0.02	0.5±0.3	0.009±0.008	
	Ni-Ni	3.11±0.02	6.0±1.0	0.007±0.005	

CN: coordination numbers; R: bond distance; σ^2: Debye-Waller factors; R-factor: goodness of fit.

The extremely short Ni-Ni distance suggests the presence of trace metallic Ni clusters, which may arise from photoreduction of highly active nanosheet regions induced by high-energy X-rays[1].

Table S2. The overpotential and Tafel slope of Ni-N4-MOF are compared with those of other representative MOF-based HER catalysts, using 1.0 M KOH as the electrolyte.

Electrocatalysts	η @ -10 mA cm^{-2}(mV)	Tafel slope (mV dec^{-1})	References
Ni-N4-MOF	363	104	This work
$Ni_{0.1}Co_{0.9}$ ZIF-67	368	109.11	Supplementary Ref.[2]
Ni-MOF@EG foil	412	117	Supplementary Ref.[3]
Ni-bit	642	190	Supplementary Ref.[4]
Co-BDC	529	111	Supplementary Ref.[5]
Cu-MOF	511	101	Supplementary Ref.[6]
Ni-BTC	683	152	Supplementary Ref.[7]
CoL1-MOF	563	75	Supplementary Ref.[8]
Cu-BIM	533	129	Supplementary Ref.[9]
$Ni_3(HITP)_2$-MOF	706	175	Supplementary Ref.[10]
CuCo-MOF	398	159.4	Supplementary Ref.[11]
HKUST-1	406	208.8	Supplementary Ref. [11]
ZIF-67	467	133.3	Supplementary Ref. [11]

II. Supplementary References

1. H. Oyanagi, Y. Orimoto, K. Hayakawa, K. Hatada, Z. Sun, L. Zhang, K. Yamashita, H. Nakamura, M. Uehara, A. Fukano and H. Maeda, Scientific Reports, 2014, 4, 7199.
2. Y. Cui, Z. Liu, H. Guo, Y. Chai, C. Liu and S. Mintova, ChemCatChem, 2019, 11, 5131-5138.
3. F. Cheng, L. Wang, H. Wang, C. Lei, B. Yang, Z. Li, Q. Zhang, L. Lei, S. Wang and Y. Hou, Nano Energy, 2020, 71, 104621.
4. L. Wang, Z. Zong, J. Wang, F. Guo, G. Huang, X. Zhang, X. Chen, Y. Fan and C. Fan, Inorganic Chemistry Communications, 2024, 170, 113217.
5. D. Zhu, J. Liu, Y. Zhao, Y. Zheng and S.-Z. Qiao, Small, 2019, 15, 1805511.
6. C. Jiao, M. Hu, T. Hu and J. Zhang, Journal of Solid State Chemistry, 2023, 322, 123978.
7. M. Nie, Z. H. Xue, H. Sun, J. M. Liao, F. J. Xue and X. X. Wang, International Journal of Hydrogen Energy, 2020, 45, 28870-28875.
8. V. Vishwakarma, N. Diyali, A. De, A. R. Choudhury and B. Biswas, ChemPlusChem, 2025, 90, e202500177.
9. S. Daniel, H. C. Kim and A. R. Podilapu, Langmuir, 2025, 41, 20734-20745.
10. A. P. Tiwari, P. Chandra, M. S. Rahman, K. A. Mirica and W. J. Scheideler, Nanoscale, 2025, 17, 11028-11036.
11. Q. Huo, X. Zhang, Y. Fu, J. Zhao, L. Fu, J. Miao, H. Sun, J. Gao and S. Liu, Research on Chemical Intermediates, 2024, 50, 107-125.